Soil-structure interaction effects on RC structures within a performance-based earthquake engineering framework

M. Mekki [1, 2], S. M. Elachachi [1], D. Breysse [1], D. Nedjar [2], M. Zoutat[2]

[1] *Université de Bordeaux, I2M / dépt. GCE, UMR CNRS S2G5 bat. B18, Av des Facultés, 33405, Talence, France.*
[2] *LM2SC, Université des Sciences et de la Technologie d'Oran, BP 1505, El M'naouar, 31000, Oran, Algérie*

mohammed.mekki@u-bordeaux1.fr, sidi-mohammed.elachachi@u-Bordeaux1.fr, denis.breysse@ u-bordeaux1.fr, djamel_nedjar@yahoo.fr, z_marie2001@yahoo.fr

Abstract:
Performance-based earthquake engineering (PBEE) has emerged as a powerful method of analysis and design philosophy in earthquake engineering. Structures are generally assumed to be fixed at their bases in the process of analysis and design under dynamic loading. Response of structures under earthquakes is strongly influenced by the soil-structure system. In soil-structure interaction (SSI) problems the ability to predict the coupled behavior of the soil and the structure is essential and requires combined soil and structure models. In the context of PBEE, this paper combines structural behavior and seismic response analysis of SSI systems. Related to SSI analysis several issues are studied, such as relative importance of soil parameters, relative foundation/soil stiffness ratio, in regards to a specified aspect of the system response (e.g., response parameters). A simplified approach is proposed to consider SSI effects on the nonlinear seismic response of a reinforced concrete structure using the nonlinear replacement oscillator considered in Aviles and Perez-Rocha, 2003. This oscillator is characterized by an effective ductility along with the known effective period and damping of the system for the elastic condition. The N2 method (Fajfar, 2000) is used to determine the nonlinear response and extended to include SSI in the design. It is confirmed that the response of the structure depends not only on its dynamic characteristics and on the seismic excitation characteristics but also on the external environment surrounding the base of the structure, i.e. the interaction between the structure, the foundation and the soil. The proposed approach is validated and compared with time history analysis, Building Seismic Safety Council (BSSC) method (NEHRP, 2003), and a method proposed by Aviles and Perez-Rocha (2003).

Key words: Soil-structure interaction; Performance based design; demand spectrum; Capacity curve; design codes; shear wave velocity.

1. Introduction

The need for improvement in the existing seismic design methodology implemented in codes has been widely recognized. The structural engineering community has developed a new generation of design procedures that incorporates performance-based engineering concepts. It has been recognized (e.g., Fajfar and Krawinkler, 1997) that damage control must become a more explicit design consideration. This aim can be achieved only by introducing some kind of nonlinear analysis into the seismic design methodology. The nonlinear static methods, nowadays allowed by many seismic codes (Eurocode 8, FEMA 356 and FEMA 368), are mainly related to two approaches available in the literature: the capacity spectrum

method proposed by Freeman (Freeman, 1998) and the N2 method proposed by Fajfar and al. (Fajfar and Gaspersic, 1996) whose denomination underlines this aspect: evaluation of the nonlinear (N) response of the structure by two (2) different numerical models (MDOF and SDOF systems).

On another hand, research and practice have shown that a structure founded on a deformable soil could respond differently compared to a fixed base one. The deformations of a structure during earthquake shaking are affected by interactions between three linked systems: the structure, the foundation, and the geologic media underlying and surrounding the foundation. A seismic SSI analysis evaluates the collective response of these systems to a specified free-field ground motion (Stewart et al., 1998). Indeed, in flexible supported case, mutual interaction between structure and adjacent soil takes place inducing modifications in the dynamic response (Menglin and al., 2011). Nevertheless, the effect of SSI may differ between linear and non linear systems. Thus, the current interaction methodologies based on elastic response studies could not be directly applicable to structures expected to behave inelastically during severe earthquakes. Consequently, ignoring the nonlinear characteristics of the SSI phenomenon could lead to erroneous predictions of structural damage.

For elastic systems, first studies for SSI were conducted by Veletsos and Meek (1974); Veletsos and Nair (1975) for surface-supported structures. In these works, the effects of the inertial SSI are summarized by an equivalent SDOF characterizing support ground flexibility and the foundation damping. The effect of the flexible soil is included by modifying the fixed base fundamental period. The foundation damping associated to radiation and soil material damping is introduced by defining an effective damping of the superstructure-foundation system as the sum of a term proportional to viscous damping in the structure and an equivalent viscous foundation damping. The increase of the natural period and the added foundation damping have been extensively studied by several authors (e.g Luco 1980; Aviles and Perez-Rocha 1996). Nevertheless, this replacement oscillator approach is strictly valid only for elastic superstructure-foundation systems. This aspect is a significant limitation in earthquake engineering, where inelastic superstructure behavior is experienced. Despite the assumption that the elastic behavior of the structure, this approach has been included in several seismic design provisions (e.g. ATC 40, 1996; FEMA 356, 2000; FEMA 450, 2003), using free-field response spectra combined with effective values of both fundamental period and equivalent viscous damping including elastic SSI.

The effects of the SSI on elastoplastic structure have not been extensively studied. Theoretical researches conducted by Priestley and Park (1987) for elastoplastic bridge piers showed that the foundation compliance reduces the ductility capacity of the system. More recently, several other studies using the replacement oscillator technique (Ciampoli and Pinto, 1995; Rodriguez and Montes, 2000 ; Aviles and Perez-Rocha, 2003) have been conducted in order to elucidate the effect of the SSI on the maximum required ductility. Similarly, Ghannad and Jahankhah (2007) performed parametric studies and revealed the importance of SSI on structural inelastic behavior. The authors indicated that the strength reduction factor R_μ of a structure has a remarkable difference between fixed base assumption and by including its foundation flexibility. Khoshnoudian and Behmanesh (2010) in their study evaluated the damping defined in FEMA 440 (2005) to include the SSI effect.

In this study, a PBEE framework which includes the SSI effects on the seismic nonlinear structural response is established. At first, the nonlinear response is determined by the N2 method for a system without considering SSI, then some significant modifications are made to include the effect of SSI. This study is aimed to formulate an approximate procedure

for the simplified analysis of nonlinear soil-structure; and to develop information that may be used in design for assessing the yield resistance and maximum deformation of interacting systems through the nonlinear analysis of fixed-base systems (Mekki and Elachachi, 2011).

2. Nonlinear analysis of soil structure interaction

Recently, building codes propose PBEE methods for new and existing structures. The most appropriate approach for performance evaluation seems to be the combination of structural capacity and seismic demand. Examples of these methods are: the capacity spectrum method applied in ATC40 (ATC 40, 1996), the displacement coefficient method used in FEMA and N2 method.

In most cases, these methods are used with the assumption of free field conditions regarding the demand spectrum and fixed base conditions regarding the capacity curve. However, it is well known that due to SSI, the response of the structure supported on a soil profile may be different from the fixed-base state. The soil structure system is in general more flexible and energy absorbing than the traditionally assumed fixed base model (Avilés and Pérez-Rocha, 2003). The SSI influences the demand and the structural capacity values as well. A PBEE framework which includes the SSI effects on the seismic nonlinear structural response must be established.

The N2 method will be used for the evaluation of the structural performance. The choice of this method is due to its simplicity, applicability and to its ability to provide structure displacement with manageable computational effort and reasonable accuracy. However, like any approximate method, N2 method is subject to several limitations. It assumes that: (a) displacement shape is constant i.e. it does not change during the structural response to ground motion, (b) the first mode is predominant. These are the basic and the most critical assumptions. N2 method is inaccurate when higher mode effects are significant, and it may not detect the structural weaknesses when the structure's dynamic characteristics change after the formation of the first plastic mechanism (Fajfar, 2000; Hemsas et al., 2010). In order to take into account the effect of SSI on nonlinear response based on N2 method, a novel approach is proposed and is illustrated in on Figure 1 it is organized in the following fundamental steps:

a. Determination of the pushover curve of a multi degree of freedom (MDOF) structure considered initially as fixed in its base. This curve is represented in terms of base-shear force versus roof displacement relationship and evaluated by monotonically increasing horizontal forces applied to the structure (pushover analysis).
b. Evaluation of seismic demand. The evaluation of the structural performance is determined by the N2 method (Fajfar, 2000) for a fixed-based system (Figure 1.b). In this method, seismic demand is determined by using response spectra in acceleration-displacement format. The pushover curve (base shear-roof displacement) is converted to a capacity curve (spectral acceleration-displacement, Figure 1.b).

Figure 1. PBEE framework including SSI

c. Introduction of SSI through impedance functions. These functions describe the stiffness and damping characteristics of the foundation-soil system. They should account for the soil stratigraphy, foundation stiffness and geometry (Figure 1.c).
d. The capacity curve of flexible base system (with SSI) is obtained by modifying the initial capacity curve built for a fixed-based structure. The intersection between the capacity curve (with SSI) and the inelastic spectra (with SSI) gives the performance point (Figure 1.d).

The efficiency of this simplified approach to readily estimate displacement will be validated by comparison with results obtained rigorously. In the following sections, each of these steps will be farther explained and developed.

3. Nonlinear response of fixed base structure by N2 method

The N2 method (Fajfar, 2000) which has been included in the Eurocode 8 (2003) is described briefly in the following. It is carried out under the subsequent steps:

a. Perform Pushover analysis, by applying a lateral load shape given by equation (1).

$$P = [M]\{\phi\} \tag{1}$$

$[M]$ is the diagonal mass matrix, and $\{\phi\}$ is the assumed displacement shape vector;

b. Transform Pushover curve base shear- top displacement $(V - u_t)$ of MDOF system to capacity curve acceleration-displacement $(S_a - S_d)$ (Figure 1b) using the following equations:

$$S_a = \frac{V}{M_1^*} \qquad S_d = \frac{u_n}{\Gamma_1 \phi_{N,1}} \tag{2}$$

$$M_1^* = \frac{\left(\sum_{j=1}^{N} m_j \phi_{j,1}\right)^2}{\sum_{j=1}^{N} m_j \phi_{j,1}{}^2} \qquad \Gamma = \frac{\sum_{j=1}^{N} m_j \phi_{j,1}}{\sum_{j=1}^{N} m_j \phi_{j,1}{}^2} \tag{3}$$

where M_1^* is the effective modal mass of the structure, related to the magnitude of the first vibration mode and to the masses m_j of different levels; $\emptyset_{j,1}$ is the amount of displacement at the level j corresponding to the first vibration mode; and Γ is modal participation factor.

c. Convert the elastic spectrum from acceleration-period format $(S_{ae} - T)$ to acceleration-displacement format $(S_a - S_d)$, and then reduce this spectrum by the reduction factor to obtain the inelastic spectrum whose parameters are obtained as follows:

$$S_{de}(T,\xi) = \frac{T^2}{4\pi^2} S_{ae}(T,\xi) \tag{4}$$

$$S_a(T,\xi) = \frac{S_{ae}(T,\xi)}{R_\mu} \tag{5}$$

$$S_d(T,\xi) = \frac{\mu}{R_\mu} S_{de}(T,\xi) = \frac{\mu}{R_\mu}\frac{T^2}{4\pi^2} S_{ae}(T,\xi) = \mu \frac{T^2}{4\pi^2} S_a(T,\xi) \tag{6}$$

$S_{ae}(T,\xi)$ and $S_{de}(T,\xi)$ are elastic spectral acceleration and elastic spectral displacement respectively, corresponding to the period T and a fixed viscous damping ratio ξ. $S_a(T,\xi)$ and $S_d(T,\xi)$ are the inelastic spectral acceleration and inelastic spectral displacement inelastic spectrum respectively. μ is the ductility defined as the ratio between the maximum displacement and the yield displacement, and R_μ is the reduction factor due to ductility. Several proposals have been made to express the reduction factor. Equation (7) represents a simple version of those proposed by Vidic et al. (1994).

$$\begin{cases} R_\mu = (\mu - 1)\frac{T}{T_c} + 1 & T < T_c \\ R_\mu = \mu & T > T_c \end{cases} \tag{7}$$

The structure displacement is associated with the position of the elastic period with respect to the soil characteristic period T_c. When T is larger than T_c the theory of equal displacements of elastic and inelastic systems in long periods range is applicable.

The top displacement of the MDOF system can be then calculated by equation (8) :

$$u_t = S_d \Gamma \tag{8}$$

4. Soil –structure interaction model

4.1. Impedance functions

The interacting soil-structure system is illustrated in Figure 1.c. The superstructure is converted into a single degree of freedom (SDOF) system with height h_{eff}, mass m, lateral stiffness k and damping c, which may be considered to be the effective values for the first mode of vibration of the structure. The three degrees of freedom include the total lateral displacement of the structure, $\tilde{u}_t$, the horizontal displacement of the foundation relative to the free-field motion, u_0, and the rotation θ of the system at the foundation level (Wolf and Deeks, 2004). The impedance function are represented by their lateral and rotational springs/dashpots with stiffness k_u and k_θ (springs), damping c_u and c_θ (dashpots) respectively,

$$k_u = \frac{8}{2-\nu} G r_u \,, \qquad k_\theta = \frac{8}{3(1-\nu)} G r_\theta^3 \tag{9}$$

$$c_u = \frac{4.6}{2-\nu} \rho V_s r_u^2 \,, \qquad c_\theta = \frac{0.4}{1-\nu} \rho V_s r_\theta^4 \tag{10}$$

where the soil is characterized by its Poisson's ratio ν, shear modulus G, and mass density ρ. The shear wave velocity for the medium is then given by $V_s = \sqrt{G/\rho}$, r_u and r_θ are the foundation radii computed separately for translational and rotational deformation modes to match the area A_f and moment of inertia I_f of the actual foundation (i.e., $r_u = \sqrt{A_f/\pi}$, $r_\theta = \sqrt[4]{4\, I_f/\pi}$).

4.2. Effective period and effective damping of the system

Veletsos and Meek (1974) found that the maximum seismically induced deformations of the oscillator in Figure 1.c could be predicted accurately by an equivalent fixed-base SDOF oscillator with period $\tilde{T}$ and damping ratio $\tilde{\xi}$. These are referred to as flexible-base parameters, as they represent the properties of an oscillator which is allowed to translate and rotate at its base. The flexible base period is evaluated from:

$$\tilde{T} = T\sqrt{1 + k\left[\frac{1}{k_u} + \frac{h_{eff}^2}{k_\theta}\right]} \tag{11}$$

where $T = 2\pi\sqrt{m/k}$ is period of the fixed-base structure. The flexible-base damping $\tilde{\xi}$ ratio has contributions from viscous damping in the structure ξ, soil damping ratio ξ_g, as well as radiation ξ_θ and hysteretic ξ_u damping in the foundation.

$$\tilde{\xi} = \frac{T^2}{\tilde{T}^2}\xi + \left[1 + \frac{T^2}{\tilde{T}^2}\right]\xi_g + \left[\frac{T_u^2}{\tilde{T}^2}\xi_u + \frac{T_\theta^2}{\tilde{T}^2}\xi_\theta\right] \tag{12}$$

where $\xi = \pi c/kT$ is the damping ratio for the fixed-base conditions; $T_u = 2\pi\sqrt{m/k_u}$ and $T_\theta = 2\pi\sqrt{m\,h^2/k_\theta}$ are the natural periods associated with rigid body translation and rocking of the structure, whereas $\xi_u = \pi c_u/(k_u\tilde{T})$ and $\xi_\theta = \pi c_\theta/(k_\theta\tilde{T})$ are the soil damping ratios for the horizontal and rocking modes of the foundation; and ξ_θ is the soil damping.

4.3. Shear-wave velocity

For seismic design in accordance with site conditions in most of design guides, the site effects are quantified according to the mean shear wave velocity V_s to a depth of 30 m ($V_{s,30}$) and the corresponding site classes. Accordingly, in the usual seismic codes, the site characterization for a site class is based only on the top 30 m of the ground. The site class is determined unambiguously by this single parameter, $V_{s,30}$. For a profile consisting of n soil and/or rock layers, $V_{s,30}$ (in units of m/s) can be given by

$$V_{s,30} = \frac{\sum_i^n h_i}{\sum_i^n \frac{h_i}{V_{si}}} \tag{13}$$

where h_i is the thickness of the ith layer between 0 and 30 m and V_{si} is the shear-wave velocity in the ith layer.

Another property which characterizes each soil category is the characteristic period of soil T_c, defined as the transition period between constant acceleration and constant velocity segment of the elastic spectrum (Figure 2.a).

Figure 2. Elastic response spectrum of Algerian seismic code (RPA, 2003) and empirical relationship between T_c and V_s

The utilized elastic response spectrum is the Algerian response spectrum (RPA, 2003). This paraseismic code is close to Eurocode 8 and it assumes that T_c (characteristic soil period) is constant for each soil type (4 types : very soft, soft, hard and rock soils). It seemed more appropriate in this study to consider a continuous variation of T_c instead of a discrete one (Figure 2.b). Equation 14 has been fitted on the central values provided by the regulations for each class and thus allows to link of the characteristic soil period at the soil shear wave velocity.

$$T_c = 3.927 V_s^{-0.3582} \tag{14}$$

where V_s is in (m/s) and T_c in seconds

4.4. Effect of V_s on effective period and damping of system

The main parameters that characterize the SSI effects are the period lengthening ratio $\tilde{T}/T$, and the shear reduction factor $\tilde{V}/V$. Figure 3 depicts the variation of $\tilde{T}/T$ versus V_s. For the evaluations shown in this figure and all the subsequent figures, a soil Poisson's ratio $\nu = 0.3$ has been selected. The effective height of the structure is equal to 7m. The case study example (described in §6), has been analyzed for various shear wave velocity V_s values ranging from 50 m/s for very soft soil conditions to 1900 m/s for a stiff soil condition.

Figure 3. Variation of $\tilde{T}/T$ with V_s.

Figure 3 shows the continuous decrease of the effective period $\tilde{T}$ when V_s values increase, due to the flexibility of the structure supports in comparison with the fixed-base structure (the $\tilde{T}/T$ ratio amounts 3.3 for $V_s = 50m/s$ and amounts 1.3 for $V_s = 200m/s$, for the medium soft soils). This is accompanied by the dissipation of a considerable amount of the vibrational energy due to the frequency-independent material damping due to the internal friction.

The effective damping $\tilde{\xi}$ of the system is significantly different from the structure damping in most of the cases. This is clearly shown in Figure (4), where the equivalent damping $\tilde{\xi}$ is plotted versus V_s for representative values of $\xi_g = 5;\ 10\ and\ 20\%$. The structural damping ratio ξ is taken equal to 5%. It can be deduced that when the soil material damping ratio ξ_g, is equal to the structural damping ratio ξ, a constant equivalent damping $\tilde{\xi}$ equal to ξ is obtained, and when ξ_g is larger than ξ the effective damping $\tilde{\xi}$ will increase for decreasing V_s. One can see that for a soil shear wave velocity of 50 m/s the effective damping is 1.86 times larger than the structure damping for $\xi_g = 10\ \%$, this ratio jumps to 3.7 for $\xi_g = 20\ \%$.

Figure 4. Variation of $\tilde{\xi}/\xi$ with V_s for different soil damping ξ_g.

5. Nonlinear response of flexible base structure by N2 method

Two important elements of seismic performance evaluation of flexible base structure are demand and capacity spectra. Demand spectrum is the representation of the severity of the ground motion while capacity spectrum depicts the ability of the structure to withstand forces of specific nature. Demand spectrum has to be modified to account for lengthening of the period or increase in the damping of the structure. So, the SSI is introduced in the N2 method by using replacement oscillator concept. Its natural period and damping ratio are defined by the effective period and effective damping ratio using Equations 11 and 12.

To fully characterize this nonlinear replacement oscillator and to account for the inelastic interaction effects, an equivalent ductility factor is defined according to Aviles and Perez-Rocha (2003), (Equation 15):

$$\tilde{\mu} = 1 + (\mu - 1)\frac{T^2}{\tilde{T}^2} \tag{15}$$

The force-displacement relationship for the actual structure and the replacement oscillator are assumed to be of elasto-plastic type. Equation 15 is obtained by equating the yield strengths and maximum plastic deformations developed in both systems under monotonic loading. One can note (Aviles and Perez-Rocha, 2003) that the values of $\tilde{\mu}$ vary from 1 to μ, so that the effective ductility of the system is lower than the allowable ductility of the structure. The effective ductility $\tilde{\mu}$ will be equal to the structural ductility μ for infinitely-rigid soil (for which ($\tilde{T} = T$) and to unity for infinitely-flexible soil (for which $\tilde{T} = \infty$).
Therefore equations (4) to (8) become :

$$\tilde{S}_{ay}(\tilde{T},\tilde{\xi}) = \frac{\tilde{S}_{ae}(\tilde{T},\tilde{\xi})}{\tilde{R}_{\mu}(\tilde{T})} \;\; ; \; \tilde{S}_{dy}(\tilde{T},\tilde{\xi}) = \frac{\tilde{T}^2}{4\pi^2}\tilde{S}_{ay}(\tilde{T},\tilde{\xi}) \tag{16}$$

In order to extend the already known concept of the reduction factor developed for fixed-base systems to SSI, a study of Avilés and Pérez-Rocha (2003) showed that the modification of the ductility factor, the structural period and the damping coefficient of fixed base structure is a reliable way to express the interaction effects on nonlinear systems. By using this approch, we have introduced the ductility factor proposed by these authors (Equation 15) in the expression of the strength reduction factor proposed by Vidic et al (1994). This formula which depends on the dynamic characteristics of the fixed base system has been adjusted to an interaction system (Equation 17). This is a more rational way to assess nonlinear strength of flexible structures.

$$\begin{cases} \tilde{R}_{\mu} = (\tilde{\mu} - 1)\frac{\tilde{T}}{T_c} + 1 & \tilde{T} < T_c \\ \tilde{R}_{\mu} = \tilde{\mu} & \tilde{T} > T_c \end{cases} \tag{17}$$

and $\tilde{u}_t = \Gamma\tilde{S}_d$ (18)

The steps involved in the application of Equation 18 can be summarized as follows (Mekki and Elachachi, 2011):

a. By use of (11), (12) and (15), compute the flexible base period $\tilde{T}$, damping ratio $\tilde{\xi}$ and ductility $\tilde{\mu}$ of the structure whose rigid-base properties T, ξ and μ are known.
b. The value of $\tilde{R}_{\mu}$ is then estimated by application of (17).

c. From the prescribed site-specific response spectrum, determine the elastic spectral response $\tilde{S}_a$ and $\tilde{S}_d$, just as if the structure were fixed at the base.

6. Case study

The proposed simplified procedure to consider the effect of soil flexibility on structural displacement value in terms of performance point will be highlighted through the following case study (figure 5).

The studied structure is a reinforced concrete frame. To model the behavior laws of concrete and steel respectively, Kent and Park model (Kent and Park, 1971) and the elasto-plastic (Menegotto and Pinto, 1973) with hardening were used.

The lateral forces distribution determined by equation (1) corresponds to the first vibration mode $\{P^T\} = [151.8;\ 303.6;\ 459.9]kN$.

The capacity curve of SDOF system with an effective mass M^*= 91.98t and a modal participation factor Γ=1.29 is obtained by equations (2) and (3). The yielding force and displacement are respectively $F_y^* = 394.64kN$ and $S_{dy} = 7.44cm$, the ultimate displacement $S_{du} = 23.48cm$, the elastic period $T = 0.83s$, the structural damping ratio $\xi = 5\%$ and stiffness $K = 5304.60kN/m$. The yielding acceleration $S_{ay} = F_y^*/M^* = 4.28m/s^2$ or 0.43 g.

Figure 5. R.C. frame (geometry, cross sections, and constitutive laws for concrete and steel).

6.1. Effect of V_s on effective strength reduction factor $\tilde{R}_\mu$

Contemporary design criteria admit the use of strength reduction factors to account for the nonlinear structural behavior. It is indeed common practice to make use of these factors for estimating inelastic design spectra from reducing elastic design spectra.

As a result of soil effects, the value of the reduction factor $\tilde{R}_\mu$ for very soft soil is different from that of a rock soil, depending mainly on the ratio between the structural fundamental period and the soil type. The reduction ratio between the reduction factor for a flexible base system and the same system on a fixed base are given in Table 1 for different soil shear wave velocities and Peak Ground Acceleration (PGA). The Table clearly shows a significant reduction for lower values of shear wave velocity and high values of PGA. For example, there is a reduction rate of 0.60 for soil with a shear wave velocity of 125 m/s with a PGA equal to 0.6g. It can be seen that soil structure interaction reduces strength reduction factors for very soft soil. Therefore, using the fixed-base strength reduction factors for interacting systems lead to non-conservative design forces therefore interaction effects cannot be neglected for very soft soils.

The flexibility of the soil-foundation system can have beneficial impact on the applied shear force at the base of the structure.

Table 1. $\widetilde{R}_{\mu}/\ R_{\mu}$ ratio for different V_s and PGA.

6.2. Effect of V_s on structural response

In order to assess the influence of the nonlinear behavior of the structure and its foundation flexibility simultaneous on the nonlinear response of the soil structure system, the response is compared with that of a fixed-base structure. Figure 6 shows the results of the studied structure for various cases:

- with fixed base conditions (Figure 6a, b, c, d) and for four soil types.
- with SSI effects (Figure 6e, f, g, h) and for four soil types.

The demand spectrum and the capacity curves for four different values of soil shear wave velocities : very soft soil (with a shear wave velocity of 125 m/s), soft soil (V_s=300m/s), hard soil (V_s=600m/s), and rock soil (V_s=1350 m/s) are shown on Figure 6, all the other parameters are kept identical. The structural damping ratio ξ is equal to 5% and the soil damping ratio ξ_g is taken equal 10%. One can note that soil shear wave velocities V_s have significant influence on both the inelastic acceleration spectrum as on well as inelastic displacement.

Figure 6. Capacity and demand spectra for different values of soil shear wave velocities: Without SSI (left) and with SSI (right) (PGA = 0.6g).

The results illustrate the significant contribution of SSI in reducing the spectrum acceleration when the relative stiffness between the structure and the soil is decreased. One can see for example that the displacement increases when soil shear wave velocity decreases (three times greater in the case of very soft soil (Figure 6.e) than in the case of rock soil (Figure 6.h)).

For very soft soil($V_s = 125m/s$), the displacement of the structure induced by the earthquake (performance point) is close to $\tilde{S}_{du}$ which is equal to 32.18cm. Thus, this structure will suffer premature failure which is due the site effect on structure. Indeed, results will show that seismic activity in a given place depends to a large extent on the nature of the soil. A spectral acceleration $\tilde{S}_a$ reduction is observed when SSI phenomenon is included. In addition, it is shown that structure built on rock soil undergoes spectral acceleration larger than on very soft soil (1.2 times greater in the case of rock soil than in the case of very soft soil) and therefore base shear force is more important as it was noted in §6.1.

Period lengthening ratio $\tilde{T}/T$, damping, $\tilde{\xi}$, spectral acceleration, $\tilde{S}_a$, ductility factor, $\tilde{\mu}$, and top displacements $\tilde{u}_t$ of soil-structure system at the performance points are given in Tables 1 and 2. The soil materiel damping ratios ($\xi_g = 10;\ 20\%$) for peak ground acceleration (0.1; 0.3 and 0.6g) are analyzed.

On Table 3 it is observed that the top displacement $\tilde{u}_t$ increases as the base condition changes from high value of V_s ($V_s = 1350m/s$) to low value of V_s ($V_s = 125m/s$). The increase in top displacement is due to the overall reduction in the global stiffness resulting from the

induced foundation movements. This trend of increase in displacement demand is also visible when looking at the displacement response spectra (Figure 6e, f, g, h).

However, for all cases, the foundation flexibility induced lateral displacements and rotations at the base of the structure may affect the ductility demand of the structure. The ductility demand is lower for lower intensity motions, but increases for higher intensity motions, as it can be expected. For low value of PGA (PGA=0.1g), none of the cases show yielding of the structure ($\tilde{\mu}$,=1, Table 3). However, it can be observed that the foundation flexibility effect on the ductility demand is always important for the lowest values of $V_s = 125m/s$.

It can be observed from table 3 that the foundation flexibility effect is a decrease of the spectral acceleration $\tilde{S}_a$, and this effect is more pronounced for the lower values of V_s (up to 71% for $V_s = 125m/s$, $\xi_g = 10\%$, and $PGA = 0.1g$). This means that SSI enhances the effect of the inelastic behavior of the structure with respect to its internal shear forces.

Table 2. $\tilde{T}/T$, $\tilde{\xi}$ for V_s and ξ_g.

Table 3. $\tilde{\mu}$, $\tilde{S}_a$ and $\tilde{u}_t$ for PGA, V_s and ξ_g

Figure 7 depicts the variation of $\tilde{u}_t/u_t$ versus V_s for two representative values of soil damping ratio ($\xi_g = 10$ and 20%). Each curve in the figure shows the top displacement of SSI system with respect to that for the fixed-base system, for to shear wave velocity values ranging from 50 m/sec to 1900 m/s. As expected, the ratio $\tilde{u}_t/u_t$ approaches unity with as light increasing values of V_s. For $V_s = 400\ m/s$, the two curves show increase of $\tilde{u}_t/u_t$. For $V_s = 50\ m/s$ and $\xi_g = 10\%$, the top displacement is 2.6 times larger than in the fixed-base case. This is primarily due to the increased system damping with increasing SSI effects. The increase of top displacement for the very soft soil and soft soil ($V_s \leq 400\ m/s$) is associated with greater energy available in the excitation around the fundamental period of the structure-soil system.

Figure 7. Variation of $\tilde{u}_t/u_t$ with V_s for different soil damping ξ_g.

7. Comparative Study

In order to assess and to qualify our approach, a comparison has been carried on between:

- the simplified proposed method,
- the method introduced in the BSSC code (NEHRP, 2003) where the roof displacement can be obtained using the following equation:

$$\tilde{u}_t = \frac{\tilde{V}}{V}\left(\frac{M_0 h_{eff}}{K_\theta} + u_m\right) \tag{19}$$

where M_0, V and u_m are respectively the overturning moment, base shear and the maximum displacement of the fixed-base structure.

- the approach proposed by Aviles and Perez-Rocha (2003). The displacement of the structure is calculated by:

$$\tilde{u}_t = u_t \frac{\tilde{\mu}}{\mu}\frac{\tilde{T}^2}{T^2} \tag{20}$$

- and a nonlinear time history method.

A set of ten synthetic accelerograms compatible with the Algerian response spectrum is used. The average of the maximum displacement is compared with that obtained by other methods.

The generated synthetic earthquakes are obtained with SIMQKE (Lestuzzi and al., 2004). This simulation is called semi-empirical compatible with the spectrum of the horizontal component of Regulation RPA99. Figure 8 shows an example of an artificial generated earthquake relative to a very soft soil.

Figure 8. Characteristics of seismic loading (generated artificial earthquake compatible with the response spectrum of RPA99-version 2003)

The analysis of the maximum displacement of the structure is performed for structure and soil damping ($\xi = 5\%$ and $\xi_g = 10\%$) and PGA of 0.4 g. The proposed approach gives good estimates of maximum top displacements of the structure in comparison with the results obtained by the BSSC method, the nonlinear time history method, and Aviles & Perez-Rocha method, as shown in Figure 9 and Table 4.

On referring to the exact dynamic method whose each point on the curve figure 9 shows the top displacement of the structure for different values of V_s, we note that the values of the maximum displacement of the structure obtained by the proposed method are very close to those of the nonlinear time history method. From these comparisons, the proposed approach provides a simple and reliable way to study the SSI effect on the nonlinear response of structures.

Figure 9. Comparison between top displacement demands determined by the proposed method, time history nonlinear, method introduced in the code BSSC and approach proposed by Aviles and Perez-Rocha (2003).

Table 4. Comparison between top displacement demands determined by four methods

8. Conclusions

In this study, the seismic performance of reinforced concrete structure is estimated considering soil structure interaction and inelastic behavior for the structure. The proposed approach presented herein can be applied in practice to any regular structure type and geotechnical environment to account for the SSI effects in earthquake resistant design of yielding structures. The approach concept is based on N2 method by determining the capacity curve of fixed based system oscillating predominantly in the first mode, and then modified to obtain the capacity curve of flexible base system by using the nonlinear replacement oscillator concept.

Results obtained through the proposed approach when compared to those of the BSSC method as well as the time history analysis, show that the simplified proposed methodology gives a good estimation of structural lateral displacement comparing to that obtained rigorously with nonlinear dynamic analysis when SSI is taking into account.

This study confirms also that an increase in damping occurs when the effect of the SSI is taken into account, which will result in a reduction of seismic demand, due to the dissipation of energy through the soil radiation and the internal damping. These two effects occur simultaneously during the seismic movement. It is thus very difficult to ignore the influence of these two phenomena.

Due to soil effects, the behavior factor value for very soft soil can be very different from that applied to rock soil, depending mainly on the ratio of the fundamental period of the structure to the predominant period of the site. For this reason it seems inappropriate to consider the same value of R_μ for both fixed and flexible structure. Accounting for this influence will assess more accurately the nonlinear response of the structure and can therefore change the design process used actually in seismic design codes.

The methodology proposed in this study has clearly brought out the effect of shear wave velocity, soil damping ratio and peak ground acceleration on the seismic performance of structure. It is also confirmed that the response of the structure depends not only on its dynamic characteristics, on the seismic excitation characteristics but also on the external environment surrounding the base of the structure, i.e. the interaction between the structure, the foundation and the soil.

9. Bibliographie

ATC-40, *Seismic evaluation and retrofit of concrete buildings, vols. 1 & 2*. Redwood City, CA: Applied Technology Council, 1996.

Avilés J. & Pérez-Rocha L. E., « Soil-structure interaction in yielding systems», *Earthquake Engineering and Structural Dynamics, 2003,* 32: 1749-1771.

Ciampoli, M., & Pinto, P., « Effects of soil-structure interaction on inelastic seismic response of bridge piers », *Journal of Structural Engineering ASCE*, 1995, 191 (5): 806-814.

EUROCODE 8, *Design of Structures for Earthquake resistance, prEN 1998-1: 200X. European Standard*, European Committee for Standardization, 2003.

Fajfar, P., « Evaluation of strength reduction factors for earthquake resistant design», *Earthquake Spectra*, 2000, 16 (3) : 573-92.

Fajfar, P., & Fischinger, M., « Non-linear seismic analysis of RC building : Implications of a case study », *European Earthquake Engineering*, 1987, (1) 31-43.

Fajfar, P, & Gaspersic, P., « The N2 method for the seismic damage analysis of RC buildings». *Earthquake Engineering and Structural Dynamics*, 1996, 25:31–46.

Freeman, S.A., « The capacity spectrum method as a tool for seismic design ». *Proceedings of the 11th European Conference on Earthquake Engineering*, Paris, France,1998.

FEMA 356, *Federal Emergency Management Agency, Prestandard and commentary for the seismic rehabilitation of buildings, FEMA 356. FEMA*, Washington, District of Columbia, 2000.

FEMA 368, *Federal Emergency Management Agency, Building Seismic Safety Council (BSSC), NEHRP Recommended Provisions for Seismic Regulations for New Buildings and Other Structures*, Washington, D.C., 2001.

FEMA 440, *Federal Emergency Management Agency, Improvement of Nonlinear Static Seismic Procedures, ATC-55 Draft*, Washington, 2005.

FEMA 450, *Federation Emergency Management Agency, NEHRP Recommended Provisions dor Seismic Regulations for New Buildings and Other Structures, Provisions, Commentary*. Report, 2003.

Ghannad, M.A., & Jahankhanh, H., « Site-dependent strength reduction factors for soil-structure systems ». *Soil dynamics and Earthquake Engineering*, 2007, 27: 99-110.

Hemsas, M., Elachachi S.M., Breysse D., « Evaluation of the seismic vulnerability of quasi symmetrical reinforced concrete structures with shear walls », *European Journal of Environmental and Civil Engineering*, 2010, 14 (5): 617-636.

Kent, D.C., & Park, R., « Flexural members with confined concrete ». *ASCE Journal of the Structural Division*, 1971, 97 (7): 1969–1990.

Khoshnoudian, F., & Behmanesh, I., « Evaluation of FEMA-440 for including soil-structure interaction », *Earthquake Engineering and Engineering Vibration*, 2010, 9: 397-408.

Lestuzzi, P., Schwab, P., Koller, M., Lacave, C., « How to choose earthquake recordings for non-linear seismic analysis of structures ». *Proceedings of 13th world conference on earthquake engineering*, Vancouver, 2004.

Mekki, M., & Elachachi, S.M., « Prise en compte de l'interaction sol structure dans le cadre d'une approche capacitive d'estimation de la performance sismique de structures en B.A. », *Rencontres de l'AUGC*, 29 au 31 Mai 2011, Tlemcen, Algerie.

Menglin, L., Huaifeng, W., Xi, C., Yongmei, Z., « Structure–soil–structure interaction: Literature review », *Soil Dynamics and Earthquake Engineering*, 2011, 31 1724–1731.

Menegotto, M., & Pinto, « Method of analysis for cyclically loaded reinforced concrete plane frames including changes in geometry and non-elastic behavior of elements under combined normal force and bending ». *Proceedings IABSE Symposium on resistance and ultimate deformability of structures acted on by well-defined repeated loads*, Lisbon, Portugal, 1973, pp. 15-22.
NEHRP, *Building Seismic Safety Council. NEHRP recommended provisions for seismic regulations for new buildings and other structures*, FEMA 450, Washington, 2003.

Priestley, M., Ordaz Park, R., « Strength and ductility of concrete bridges columns under seismic loading ». *ACI Structural Journal*, 1987, 84 (1): 61–76.

Rodriguez, M., Ordaz Montes, R., « Seismic response and damage analysis of building supported on flexible soils ». *Earthquake Engineering and Structural Dynamics*, 2000, 29: 647-665.

RPA, *Règles parasismiques algériennes-Version 2003*, Centre national des recherches appliquées en génie parasismique, 2003.

Stewart, J.P., Seed, R.B., and Fenves, G.L., « Empirical Evaluation of Inertial Soil Structure Interaction Effects », *Research Rep. PEER-98/07, UCB, 1998.*

Veletsos, A., & Meek, J., « Dynamic behavior of building-foundation systems ». *Earthquake Engineering and Structural Mechanics*, 1974, 3:121–138.

Veletsos, A., and Nair, V., « Seismic interaction of structures on hysteretic foundations ». *Journal of the Structural Division (ASCE)*, 1975, 101:109–129.

Vidic, T., Fajfar, P, Fishinger, M., « Consistent inelastic design spectra: strength and displacement », *Earthquake Engineering and Structural Dynamics*, 1994, 23: 502–521.

Wolf, J.P., & Deeks, A.J., *Foundation Vibration Analysis: A Strength-of-Materials Approach*, Elsevier Linacre House, Jordan Hill, Oxford, 2004.

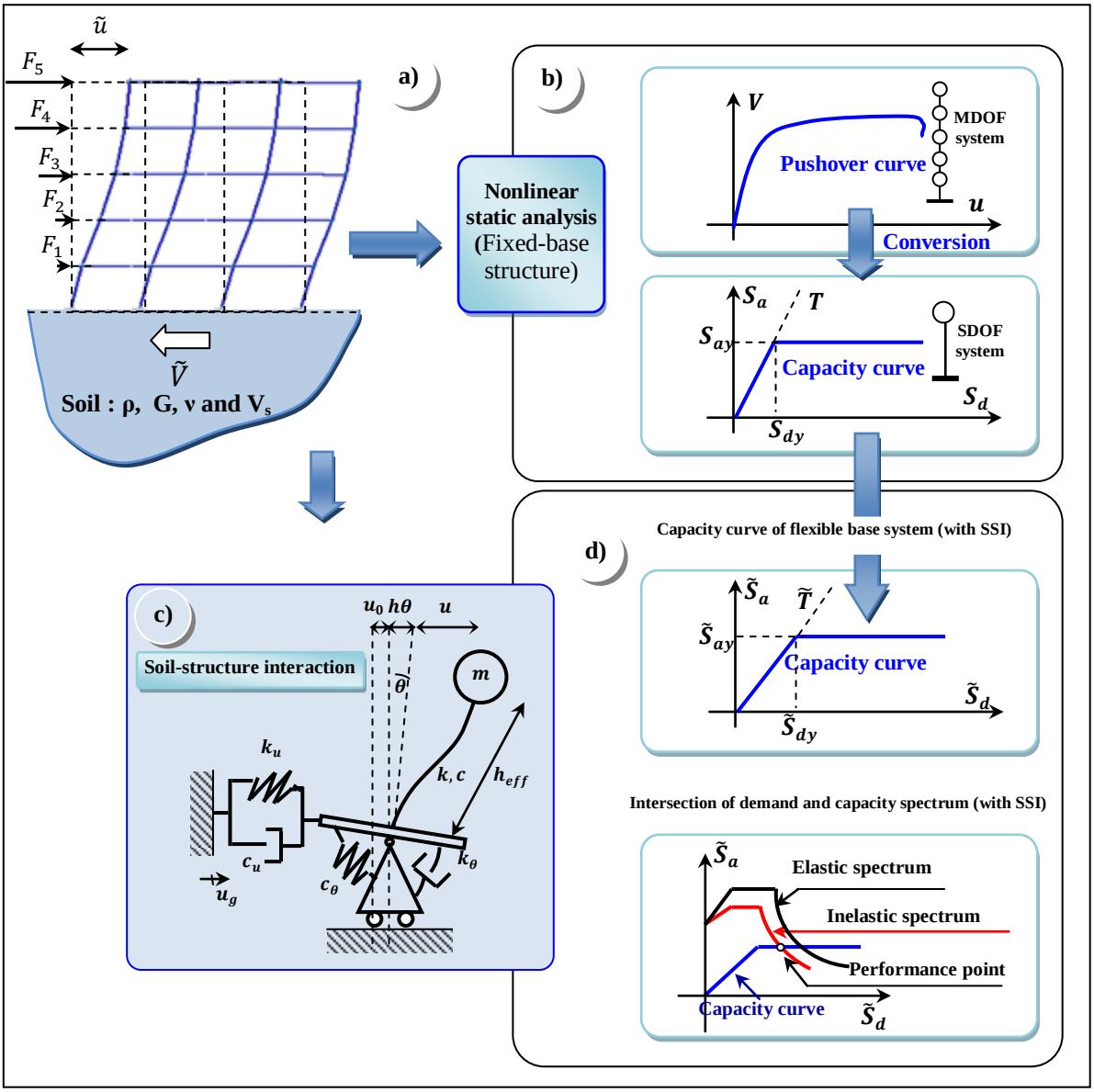

Figure 1. PBEE framework including SSI

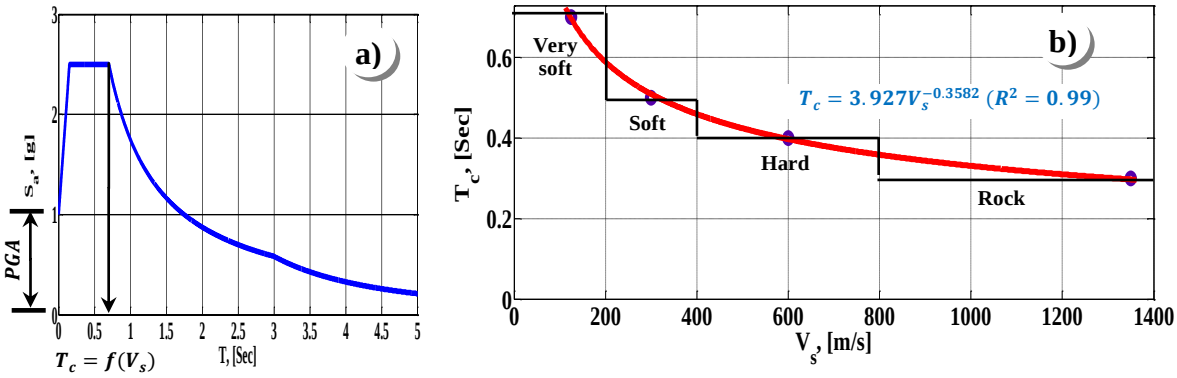

Figure 2. Elastic response spectrum of Algerian seismic code (RPA, 2003) and empirical relationship between T_c and V_s

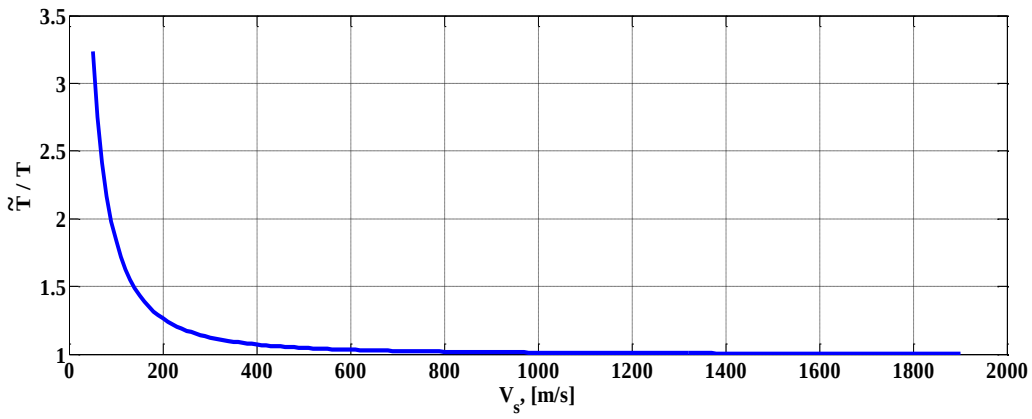

Figure 3. Variation of $\tilde{T}\ /T$ with V_s.

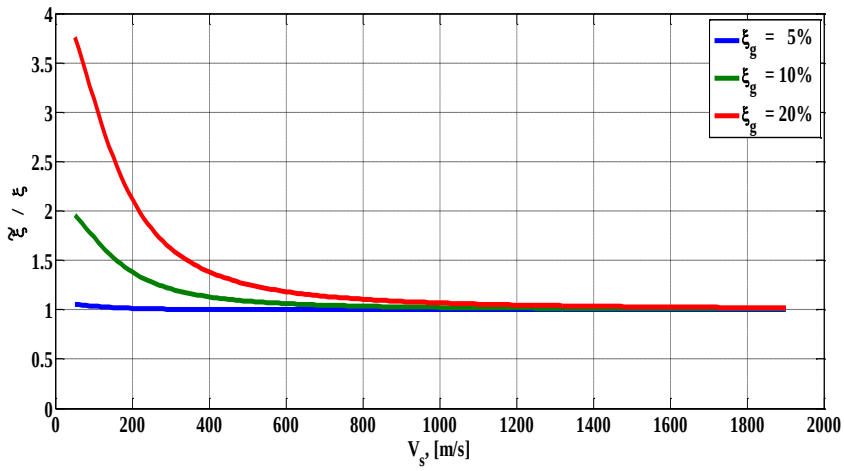

Figure 4. Variation of $\tilde{\xi}/\xi$ with $\boldsymbol{V_s}$ for different soil damping $\boldsymbol{\xi_g}$.

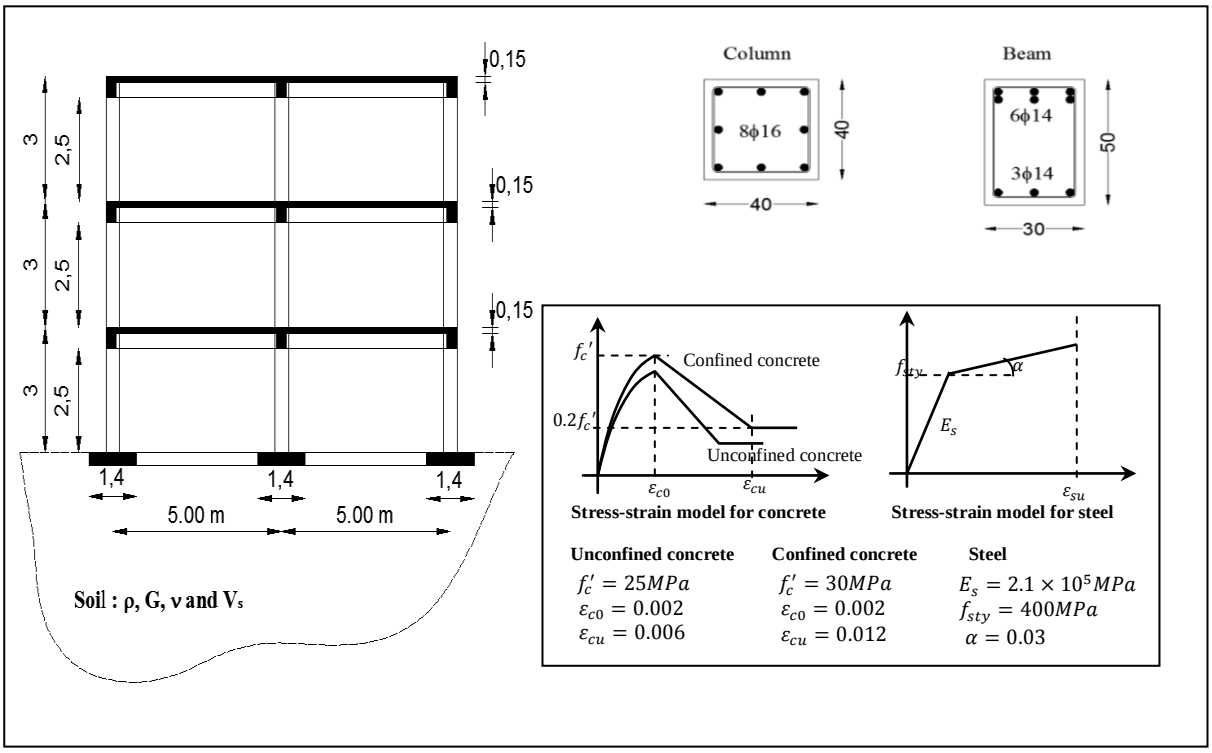

Figure 5. R.C. frame (geometry, cross sections, and constitutive laws for concrete and steel).

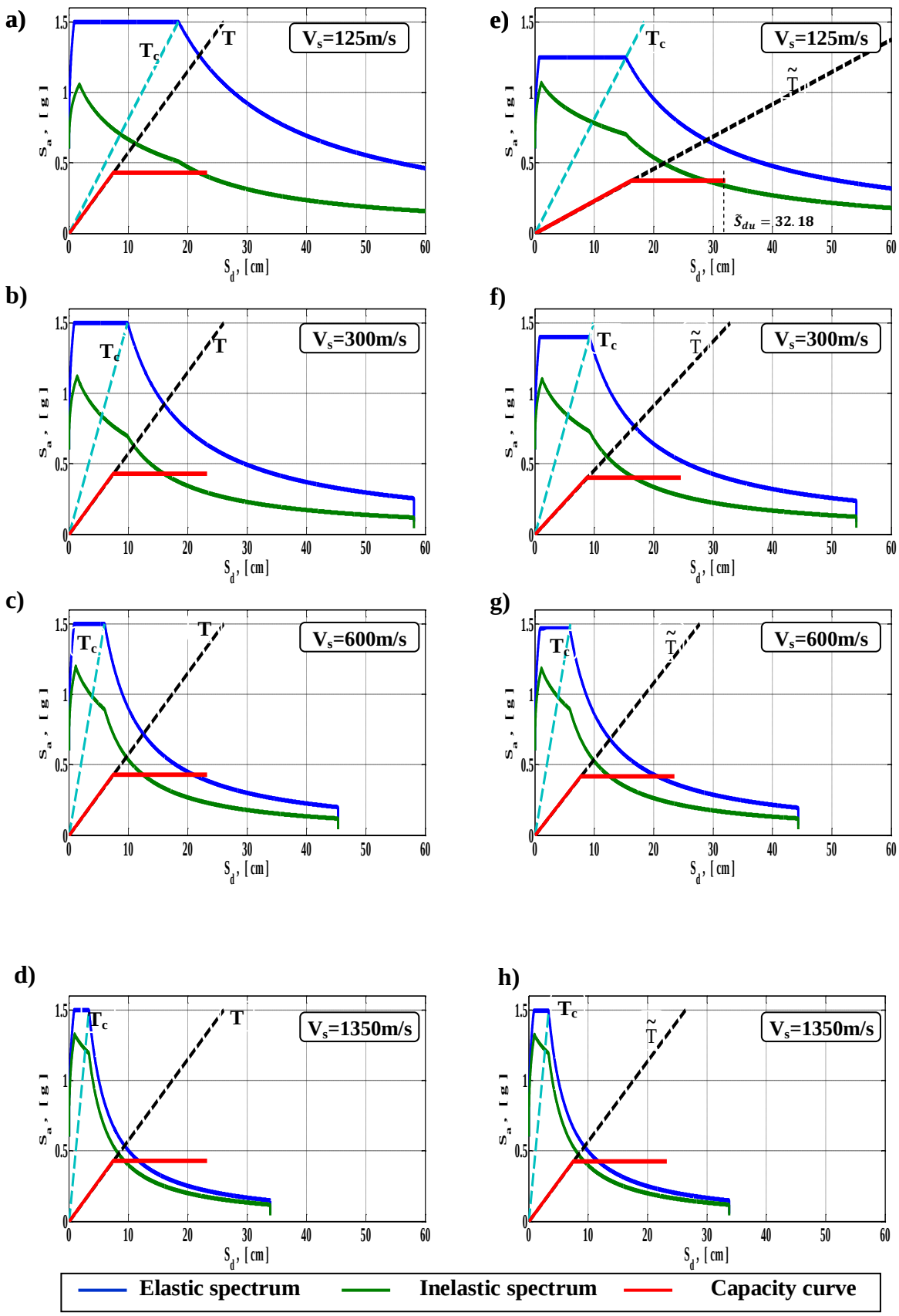

Figure 6. Capacity and demand spectra for different values of soil shear wave velocities: Without SSI (left) and with SSI (right) (PGA = 0.6g).

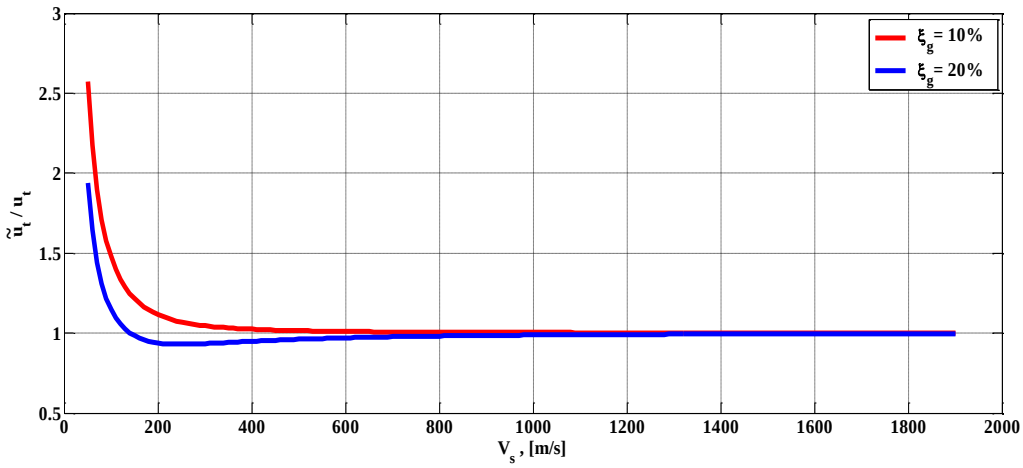

Figure 7. Variation of $\tilde{u}_t / u_t$ with V_s for different soil damping ξ_g.

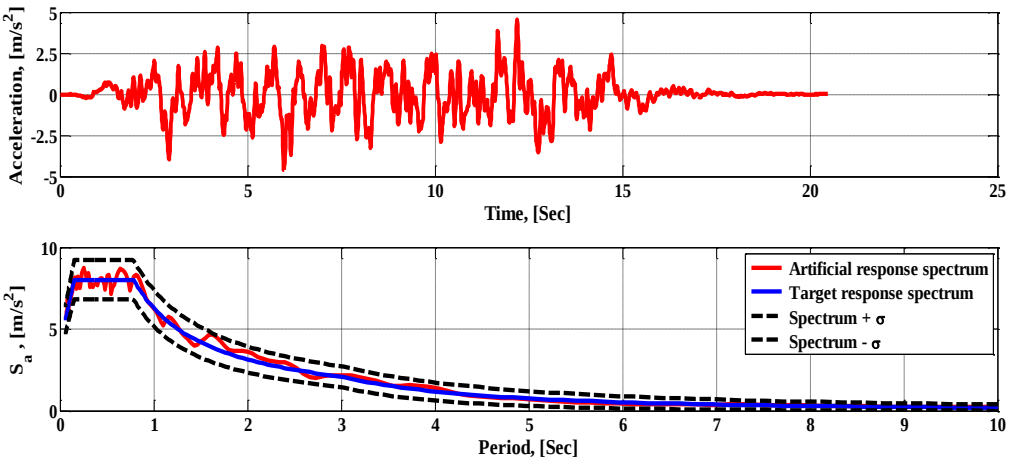

Figure 8. Characteristics of seismic loading (generated artificial earthquake compatible with the response spectrum of RPA99-version 2003)

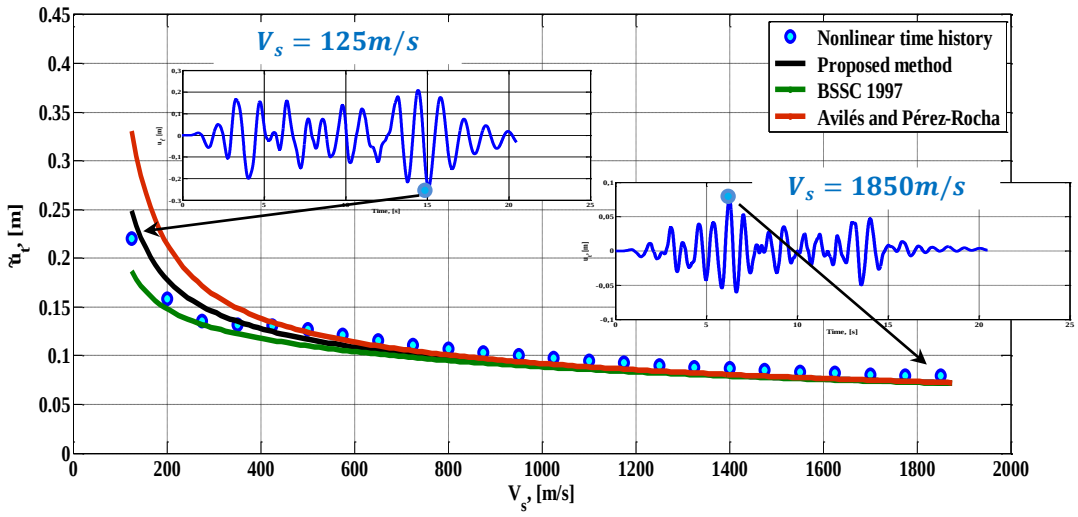

Figure 9. Comparison between top displacement demands determined by the proposed method, time history nonlinear, method introduced in the code BSSC and approach proposed by Aviles and Perez-Rocha (2003).

Table 1. $\widetilde{R}_{\mu}/\ R_{\mu}$ ratio for different V_s and PGA.

PGA, [g]	$\boldsymbol{V_s}, [\boldsymbol{m/s}]$			
	125	**300**	**600**	**1350**
0.1	1.00	1.00	1.00	1.00
0.3	0.80	0.98	1.00	1.00
0.6	0.60	0.88	0.97	1.00

Table 2. $\widetilde{T}/T$, $\tilde{\xi}$ for V_s and ξ_g.

$V_s\ (m/s)$	$\widetilde{T}/T$	$\tilde{\xi}$ (%)	
		$\xi_g = 10\%$	$\xi_g = 20\%$
125	1.58	8.10	14.10
300	1.12	6.10	8.10
600	1.03	5.30	5.90
1350	1.00	5.10	5.20

Table 3. $\tilde{\mu}$, $\tilde{S}_a$ and $\tilde{u}_t$ for PGA, V_s and ξ_g

PGA (g)	$V_s\ (m/s)$	$\tilde{\mu}$	$\tilde{S}_a(g)$		$\tilde{u}_t\ (m)$	
			$\xi_g = 10\%$	$\xi_g = 20\%$	$\xi_g = 10\%$	$\xi_g = 20\%$
0.1	**125**	1.000	0.293	0.293	0.062	0.049
	300	1.000	0.347	0.310	0.036	0.032
	600	1.000	0.396	0.381	0.027	0.026
	1350	1.000	0.413	0.410	0.020	0.020
0.3	**125**	1.200	0.293	0.293	0.186	0.148
	300	1.075	0.354	0.316	0.109	0.097
	600	1.000	0.396	0.381	0.082	0.079
	1350	1.000	0.413	0.409	0.061	0.060
0.6	**125**	1.801	0.343	0.293	0.310	0.246
	300	1.944	0.383	0.342	0.181	0.162
	600	1.664	0.404	0.387	0.136	0.131
	1350	1.273	0.414	0.410	0.101	0.100

Table 4. Comparison between top displacement demands determined by four methods

$V_s, [m/s]$		**125**	**300**	**600**	**1350**
$\tilde{u}_t, [m]$	**Nonlinear time history**	0.2414	0.1383	0.1092	0.0838
	Proposed method	0.2472	0.1437	0.1081	0.0802
	BSSC	0.1840	0.1271	0.1032	0.0794
	Aviles and Perez-Rocha	0.3301	0.1629	0.1141	0.0818